



OPEN Paleoenvironments of Late Devonian tetrapods in China

Xuelian Guo¹, Gregory J. Retallack²✉ & Jinhao Liu¹

The major evolutionary transition from fish to amphibian included Late Devonian tetrapods that were neither fish nor amphibian. They had thick necks and small limbs with many digits on elongate flexuous bodies more suitable for water than land. Habitats of Devonian tetrapods are of interest in assessing selective pressures on their later evolution for land within three proposed habitats: 1, tidal flats, 2, desert ponds, and 3, woodland streams. Here we assess paleoenvironments of the Late Devonian tetrapod *Sinostega* from paleosols in Shixiagou Canyon near Zhongning, Ningxia, China. Fossil tetrapods, fish, molluscs, and plants of the Zhongning Formation are associated with different kinds of paleosols, representing early successional vegetation, seasonal wetlands, desert shrublands, and riparian woodlands, and paleoclimates ranging from semiarid moderately seasonal to monsoonal subhumid. The tetrapod *Sinostega* was found in a paleochannel of a meandering stream below a deep-calcic paleosol supporting well drained progymnosperm woodland in a monsoonal subhumid paleoclimate. This habitat is similar to that of the tetrapods *Densignathus*, *Hynnerpeton*, and an indeterminate watcheriid from Pennsylvania, USA. Chinese and Pennsylvanian Late Devonian tetrapods lived in productive woodland streams, choked with woody debris as a refuge from large predators. Habitats of other Devonian tetrapods have yet to be assessed from studies of associated paleosols as evidence for their ancient climate and vegetation.

Although incompleteness of the fossil record of early vertebrate colonization of the land is lamentable¹, persistent attention to rare fossils and their sedimentary context have revealed intermediate forms within other major evolutionary transitions such as dinosaur to bird² and ape to human³. The late Jenny Clack proposed an extended phase of Late Devonian tetrapods intermediate within the evolutionary transition from fish to amphibian⁴. Basal tetrapods *Ichthyostega* and *Acanthostega* from Greenland were medium sized (0.5–1 m long) with long sinuous bodies, lateral line canals, and short limbs inadequate for rapid locomotion on land^{1,4}. High-carriage, fully terrestrial, tetrapods evolved much later during the Early Carboniferous⁴. Late Devonian was also a culmination of Middle Devonian evolution of progymnosperm and cladoxyl forests⁵, so that short multidirectional limbs of basal tetrapods may have been exaptations for navigating and hiding in woody debris of streams, rather than adaptations to walking or hauling on land⁶. Alternatively these stumpy limbs have been regarded as adaptations for hauling out of shrinking desert ponds⁷, or on the slimy mud of tidal flats⁸.

This paper evaluates these alternative scenarios from evidence of Late Devonian paleosols at a tetrapod locality in China (Fig. 1). The Chinese Late Devonian tetrapod *Sinostega*⁹ is based on an almost complete jaw from the Zhongning Formation in Shixiagou Canyon, northeast of Zhongning County, Ningxia Hui Autonomous Region (222 m in Fig. 2). The size of a complete *Sinostega* animal can be estimated at a little more than 0.63 ± 0.1 m from the size of its jaw relative to other early tetrapods known from complete skeletons⁶. *Sinostega* was thus similar in size to the Famennian Greenland tetrapod *Acanthostega*, which it most resembles⁹. *Sinostega* was part of an evolutionary radiation of Devonian tetrapodomorphs^{10–23}, and about the same geological age as *Ichthyostega*, *Acanthostega*, *Densignathus*, *Hynnerpeton*, and *Metaxygnathus* (Table 1). Like these other tetrapods, *Sinostega* may have had larger pelvis, sacrum and digits than Frasnian *Tiktaalik*²⁰, but lacked the short body and high carriage of *Tulerpeton*¹⁰ and Carboniferous amphibians⁴.

Other fossils from the Zhongning Formation (Supplementary Information Table S1), include the Givetian to Frasnian progymnosperm tree *Archaeopteris macilenta*, represented by rare leafy twigs (Fig. 3b) as well as abundant woody root traces (Fig. 3d–e). We consider *A. macilenta* a senior synonym of “*Sphenopteris taihuensis*”, previously recorded from the Zhongning and Shixiagou Formations²⁴. Also notable is *Ningxiaphyllum trilobatum*²⁴, lobed cupules with three dense ovoid bodies comparable with the late Famennian early seed fern *Archaeosperma arnoldi* from Pennsylvania²⁵. Sinolepid fishes in the Zhongning Formation also are evidence of late Famennian age²⁶. Oxygen and sulfur stable isotopic composition of Famennian sarcopterygian and placoderm fish from

¹Key Laboratory of Western China's Mineral Resources of Gansu Province, School of Earth Sciences, Lanzhou University, Lanzhou 730000, People's Republic of China. ²Department of Earth Sciences, University of Oregon, Eugene, OR 97403-1272, USA. ✉email: gregr@uoregon.edu

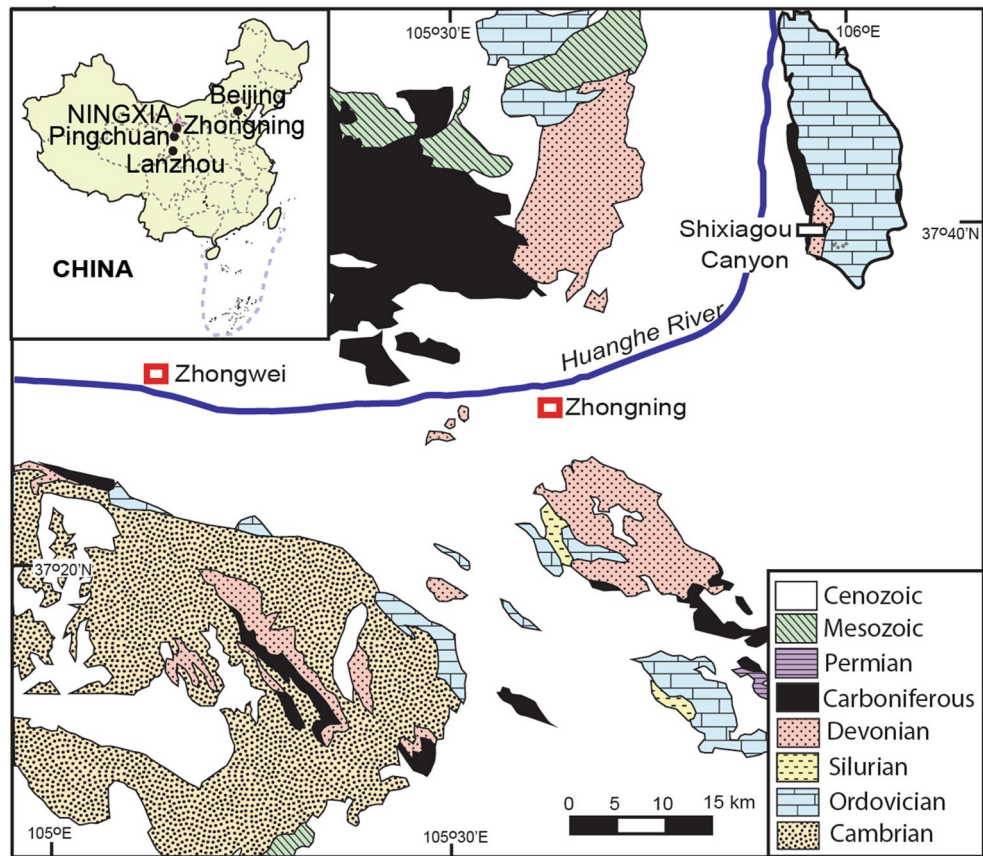


Figure 1. Late Devonian tetrapod locality and Shixiagou Canyon section near Zhongning, Ningxia Hui Autonomous Region, China. Geological map has been simplified³⁴.

Shixiagou reveal that they lived in estuaries of mixed salinity, or returned to streams from the sea to spawn, but that study did not analyse the tetrapod *Sinostega*²⁷.

Results

Ancient soilscapes

Both the Zhongning and Shixiagou Formation in Ningxia and the Shaliushui Formation near Pingchuan in Gansu²⁸ are long sequences of superimposed red calcareous paleosols (Fig. 3), similar to sequences of Late Devonian paleosols of Pennsylvania and New York^{5,6}. Interbedded with the paleosols are sandstone palaeochannels, such as the tetrapod bed itself, with cut banks as deep as 2 m (Fig. 3a). The deepest parts of the incised tetrapod fluvial palaeochannel return at a wavelength of 11.5 m laterally along outcrop (Fig. 3a), as evidence of a sinuous meandering stream, like those found elsewhere in Middle to Late Devonian red beds⁵.

The main effort of our study was to document and then interpret the variety of paleosols in a long geological section (Fig. 2), measured in Shixiagou Canyon (from narrows at N37.654774° E105.9983626° to tetrapod locality at N37.654735° E105.994513°). Six distinct kinds of paleosol encountered were given descriptive pedotype names using the indigenous Dongxiang language²⁹, and their description and interpretation is detailed in supplementary information online Tables S2 and S3. In summary, some pedotypes are very weakly developed, shaley (Ninkian) or sandy (Xulan), or weakly developed (Gieren), with much lamination, ripple marks and other sedimentary features persisting, despite partial disruption by root traces. Their root traces are mostly deeply reaching as evidence of good drainage, but one Ninkian profile had dichotomizing drab-haloed rhizomes confined to one horizon as if waterlogged (Fig. 3c). These profiles represent early successional vegetation of habitats disturbed by regular flooding such as levees and point bars^{5,12}. Other profiles are characterized by pedogenic carbonate nodules that are shallow (< 40 cm) within profiles on conglomerate (Zuzan) or siltstones (Tedzhu: Fig. 3d), or deep (> 40 cm) within the profiles below a clayey siltstone horizon (Fugun, Fig. 3e). These three calcareous pedotypes have abundant, stout, deeply-reaching root traces (Fig. 3d–e) as evidence for woody vegetation of progymnosperms or pteridosperms in well established communities stable for the many thousands of years needed to create such large nodules³⁰. Most of the calcareous paleosols have shallow calcic horizons, but 7 stratigraphic levels have paleosols with deep-calcic horizons (Fig. 2). The bed with the tetrapod *Sinostega pani* is in the uppermost of these exceptional, deep-calcic, paleosol horizons.

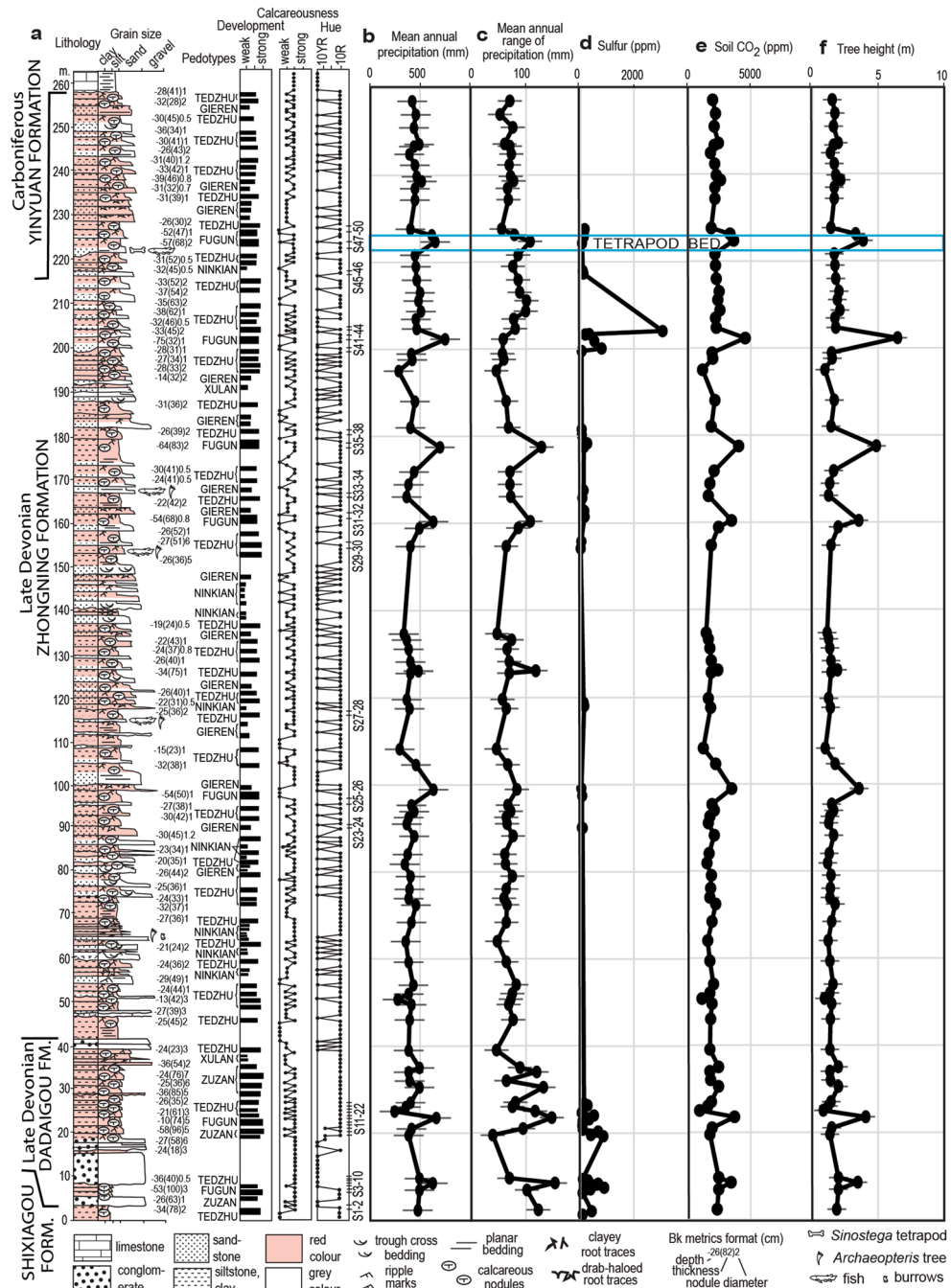


Figure 2. Geological section and paleoclimatic proxies for the Late Devonian Zhongning Formation of China: (a) measured section noting levels and degrees of development of paleosols, reaction with HCl and Munsell hue; (b) Mean annual precipitation (mm) estimated from compaction-corrected depth to calcic horizon^{30,32} (c) Mean annual range of precipitation (mm) from compaction-corrected thickness of calcic horizon^{30,32} (d) sulfur (ppm) analysed by XRF; (e) Soil CO₂ (ppm) and (f) tree height (m), both estimated from compaction-corrected depth to calcic horizon^{5,31}. Data sources are supplementary Information Tables S1–S4).

Ancient vegetation

Paleoclimate and vegetation of deep-calcic paleosols can be quantified by a variety of measurements of the paleosols (Fig. 2b–c,e–f), such as calcic horizon proxies for vegetation stature⁵ and productivity³¹, and chemical composition as proxies for mean annual precipitation and temperature³². Modern soils with deeper calcic horizons have taller trees⁵ and higher soil respiration of CO₂ as an index of secondary productivity³¹. The relationship of Devonian progymnosperm tree height to soil carbonate depth differs from modern seed plants⁵, and for estimates of past height needs correction for burial estimated from local stratigraphic thickness and vitrinite reflectance of coal in overlying beds^{33–36}. By this metric (see Methods), progymnosperms of the two deep calcic (Fugun) paleosols near the tetrapod level were 6.5 ± 0.7 m and 3.9 ± 0.7 m tall. This was a woodland rather than

Age	Ma	Taxon	Locality	References
Famennian	360	<i>Tulerpeton curtum</i>	Andreyevka, Russia	10
	363	<i>Acanthostega gunnari</i> , <i>Ichthyostega</i> sp. indet	Gauss Halvø, Greenland	11
	366	<i>Ichthyostega stensioei</i>	Gauss Halvø, Greenland	11
	366	<i>Densignathus rowei</i> , <i>Hynerpeton basseti</i> , <i>Whatcheeriid</i>	Hyner, Pennsylvania	12
	366	<i>Metaxygnathus denticulatus</i>	Bunduburrah, New South Wales	13
	366	<i>Sinostega pani</i> , <i>Hongyu chowi</i>	Shixiagou, China	9,14
	366	cf. <i>Ichthyostega</i> indet	Strud, Belgium	11
	366	<i>Ventastega curonica</i>	Ketleri, Latvia	11
	366	<i>Ventastega curonica</i>	Pavāri, Latvia	11
	370	<i>Jacobsonia livnensis</i>	Gornostayeveka, Russia	15
	370	<i>Tutusius umlambo</i> , <i>Umzantsia amazana</i>	Waterloo Farm, South Africa	16
	372	Tetrapoda indet	Plucki, Poland	17
	372	<i>Parmastega aelidae</i>	Sosnogorzsk, Russia	18
Frasnian	373	<i>Obruchevichthys gracilis</i>	Novgorod, Russia	19
	373	<i>Obruchevichthys gracilis</i>	Velna-Ala, Latvia	19
	375	<i>Elginerpeton pancheni</i>	Scat Craig, Scotland	19
	377	<i>Tiktaalik roseae</i>	Blind Fiord, Nunavut	20
	379	<i>Gogonasmus andrewsae</i>	Gogo, Western Australia	21
	379	<i>Panderichthys rhombolepis</i> , <i>Livoniana multidentata</i>	Lode, Latvia	22
Givetian	380	<i>Elpisostege watsoni</i>	Miguasha, Quebec	23

Table 1. Devonian tetrapodomorph skeletal remains in temporal order.

forest in some classifications³⁷, in strong contrast to desert shrubland heights of 0.9–2.2 m for the many shallow calcic (Tedzhu and Zuzan) paleosols in the same sequence (Figs. 2, 3a).

This indication of woodlands around streams at the Chinese tetrapod locality can be supplemented with estimates from paleosols of secondary soil productivity³¹ as respired CO₂ from compaction-corrected depth to calcic horizon. By this proxy, communities of the two deep calcic (Fugun) paleosols near the tetrapod level had high CO₂ levels of 7228 ± 588 ppm and 9101 ± 588 ppm, whereas desert shrublands of the many shallow calcic (Tedzhu and Zuzan) paleosols had only 1763 ± 588 ppm to 5128 ± 588 ppm (Fig. 2e). Woodlands with tetrapods and taller trees were more productive than usual during accumulation of the rest of the Zhongning Formation.

Ancient climate

Part of the explanation for transiently increased productivity was increased mean annual precipitation and mean annual temperature, which can be estimated from chemical index of alteration without K₂O and alkali index (see Methods) from chemical analysis of non-calcareous parts of paleosols³². Unfortunately, only two of the analysed specimens have CaO low enough to apply these proxies (Supplementary Information Table S5), but they give subhumid (692 ± 181 and 858 ± 181 mm) precipitation and temperate (5.0 ± 4.4 and 4.8 ± 4.4 °C) temperatures for paleosols at 19.6 and 20.8 m (in Fig. 2). This is cool for an estimated tropical palaeolatitude (0.9 ± 8.8°) for the Zhongning Formation³⁸, and this location may have been at high elevation during Late Devonian mountain-building to the south³⁴.

Supporting indications of subhumid precipitation and of high mountains nearby come from measurements of carbonate nodules corrected for compaction. Depth to carbonate nodules is also related to mean annual precipitation (MAP)³⁰, and thickness of carbonate nodular horizon is related to mean annual range of precipitation (MARP), or difference between wettest and driest month. The two deep-calcic (Fugun) paleosols near the tetrapod horizon have subhumid MAP of 651 ± 147 and 749 ± 147 mm, and moderately monsoonal MARP of 108 ± 22 mm and 100 ± 22 mm, whereas the numerous shallow-calcic (Tedzhu and Zuzan) paleosols have semi-arid MAP (246 ± 147–516 ± 147 mm) and non-monsoonal MARP (39 ± 22–94 ± 22 mm).

Discussion

Transients of deep calcic paleosols at irregular intervals within long sequences of shallow calcic paleosols have been found in other parts of the world, such as Devonian of Australia³⁹ and New York-Pennsylvania^{5,6}, Permian–Triassic of South Africa⁴⁰ and Utah⁴¹, and Cretaceous of China⁴² and Nevada⁴¹. In all of these cases, deep calcic levels are correlative with global CO₂ greenhouse spikes, and named marine black shales, such as 366 Ma annulata event⁸, which may correlate with the Shixiagou tetrapod site. They are considered to represent massive atmospheric pollution by CO₂ and CH₄ from basaltic eruptions of Large Igneous Provinces. In the case of late Famennian, large basaltic eruptions of the Dniepr–Donetz Rift in Ukraine may be to blame⁴³. A volcanic component to the deep calcic spikes at the tetrapod locality near Zhongning is indicated by anomalous enrichment of sulfur (Fig. 2d), mercury and chlorine⁴⁴ (Supplementary Information Tables S5–7). While massive eruption may explain the rapid onset of greenhouse spikes, their abatement requires exceptional carbon burial by geographic expansion of more productive warm-wet communities and soils polewards and into deserts⁴⁵. Woodlands with

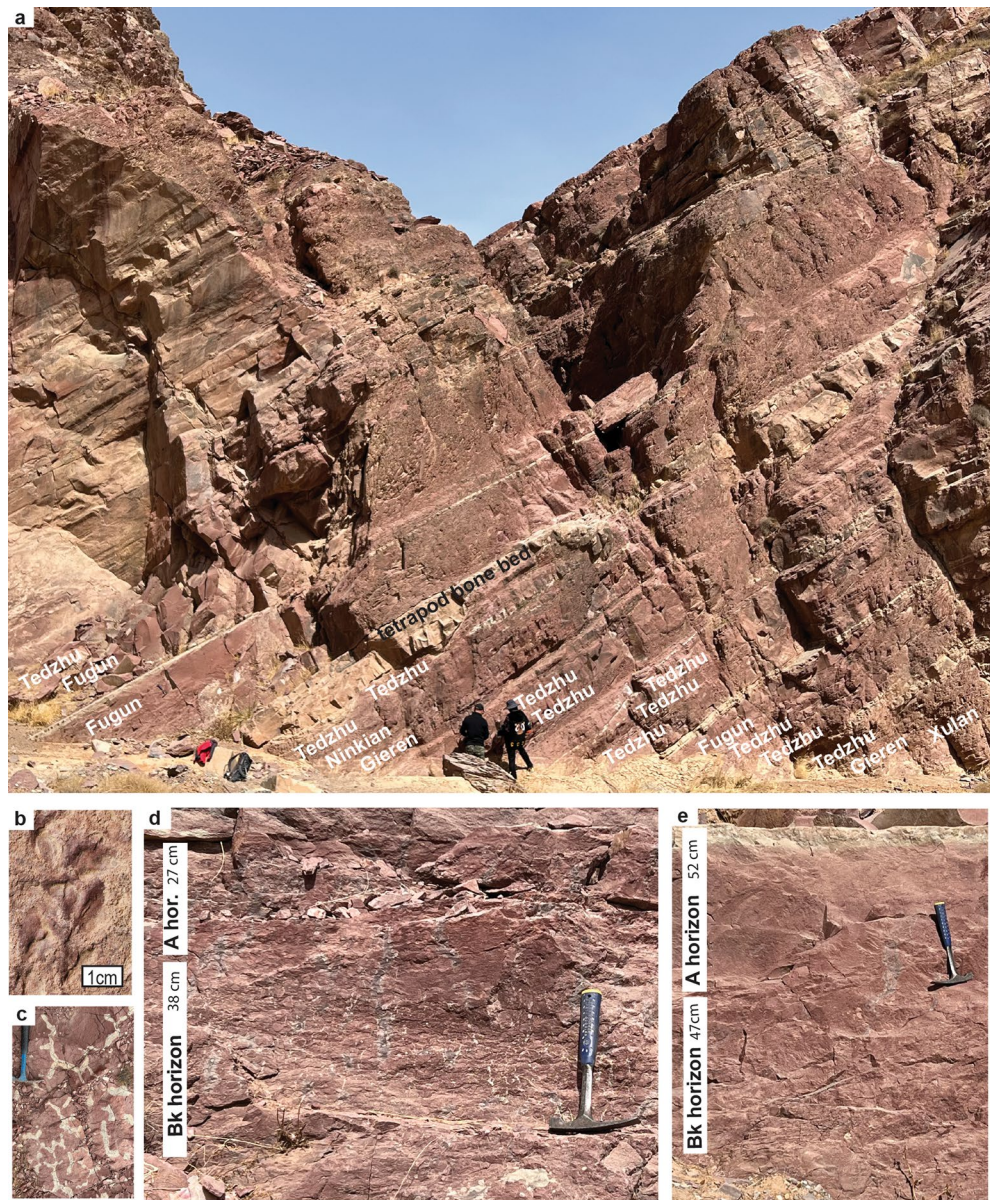


Figure 3. Field photos of Late Devonian paleosols and root traces in the Zhongning Formation of China; (a) sandstone paleochannel yielding the tetrapod *Sinostega pani*⁹, and paleosols above and below in Shixiagou Canyon; (b) progynospERM short shoot of *Archaeopteris macilenta* (63 m in Fig. 2); (c) drab-haloed dichotomizing rhizome system (– 10 m below Fig. 2); (d) shallow-calcic paleosol of Tedzhu pedotype (91 m in Fig. 2); (e) deep-calcic paleosol of Fugun pedotype (222 m in Fig. 2).

tetrapods presumably existed in more humid regions upslope and to the west throughout deposition of the Zhongning Formation, but only during these greenhouse spikes did they expand geographically into the area currently in Shixiagou Canyon.

Comparable studies of paleosols associated with other basal tetrapods remain to be completed, but existing evidence is compatible with the view that they were largely aquatic creatures of meandering streams in productive semiarid to subhumid woodlands, venturing onto land only during floods and the wet season^{6,46}. Desert shrubland paleosols also were found in the Devonian⁵, but evidence presented here and elsewhere^{6,8}, suggest that basal tetrapods avoided them. There is also isotopic, sedimentary, and paleontological evidence of Devonian tetrapods in intertidal to estuarine settings^{1,11,16,27}. Middle Devonian (Eifelian, ca 392 Ma) trackways from Zachemie in Poland have been used to argue for intertidal tetrapod habitats⁸, but these lack digits and gait of genuine tracks, and are more like fish feeding traces⁴⁷. Zachemie paleoenvironment has been reinterpreted as lakes and floodplain, rather than intertidal^{48,49}. Similar doubts have been voiced about Middle Devonian (Givetian, ca 382 Ma) Valentia Island trackways of Ireland⁵⁰, which have body drag marks, and are similar to terrestrial locomotion trails of lungfish^{51,52}.

The woodland hypothesis⁶ links Late Devonian tetrapod evolution to Middle to Late Devonian evolution of forests^{5,46,53}. Newly evolved forests changed fluvial hydrology for fish and amphibians, because trees stabilized banks to create meandering, perennial, deep streams, rather than braided, ephemeral, shallow streams^{5,46}. Paleosols and palaeobotany of the tetrapod bed near Zhongning are remarkably similar to those of tetrapod localities in Pennsylvania^{6,8}, also in streams flanked and littered with dry woodland debris, like modern creeks in outback New South Wales, Australia (Fig. 4a). Woody debris in and around streams improved fish and amphibian diversity and abundance with alternating slow and fast-flowing sections, and cooler and deeper pools^{54–56}. Tetrapods could have navigated woody debris with their small limbs in order to avoid predation from much larger fish such as *Hongyu*¹⁴ (Fig. 4b) and *Hyneria*¹² found in the same deposits. In modern streams and lakes, salamanders take refuge from predation by fish in woody debris^{57,58}. The importance of woody debris for modern amphibians is now increasingly appreciated from studies of human deforestation^{57,58}. Woody debris may have been critical to early amphibian evolution.

Methods

The main activity of this project was measuring a detailed section of paleosols by the method of eyeheights adjusted by cosine from dip of 30°W on strike azimuth 184° (Fig. 2). Three key features were recorded: (1) destruction of sedimentary bedding and size of pedogenic carbonate nodules as proxies for soil development, (2) reaction with 0.1 M HCl as a proxy carbonate content, and (3) Munsell hue as a record of chemical oxidation. Depth and thickness of the calcic horizons were also measured in the field (Bk metrics of Fig. 2 and Supplementary Information Table S4). No experiments with animals were part of this research. All data generated are included within this article.

Six distinct kinds of paleosols, or pedotypes, were recognized in the field (Supplementary Information Tables S2–3). Major and trace element concentrations were measured using XRF spectroscopy. Each XRF measurement was on a compacted disk, derived from whole-rock powder sieved to 200 µm mesh and weighing at 4 g, on a VP-320 XRF spectrometer. Mercury (Hg) was analysed by atomic fluorescence spectrometry. The relative standard deviation is about 1% (Supplementary Information Tables S4–7).

The relationship between jaw length (J in mm) and body length (L in m) of complete skeletons of early tetrapods⁶ was calculated using Eq. 1 ($n=6$, $r^2=0.98$, $s.e.=\pm 0.05$, $p=0.006$).

$$L = 0.0056J - 0.017 \quad (1)$$

Progymnosperm tree height was calculated from Eq. 2 ($n=9$, $r^2=0.95$, $s.e.=\pm 0.7$, $p=0.00002$). Depth to carbonate (D in cm) in this equation needs to be corrected for compaction³³ (C in %) due to burial (B in km) using Eq. 3 based on 1 km up-section to Ningxia coal³⁴ with vitrinite reflectance of 0.74%³⁵, so suffered about 3 km burial depth³⁶.

$$H = 0.6351e^{0.0182D} \quad (2)$$

$$C = \frac{-0.62}{\left\{ \left(\frac{0.38}{e^{\frac{B}{0.17}}} \right) - 1 \right\}} \quad (3)$$

Paleosols can be used to infer secondary soil productivity as respired CO₂ (S in ppm) estimated from compaction-corrected (Eq. 3) depth to calcic horizon (D in cm) using Eq. 4 ($n=17$, $r^2=0.54$, $s.e.=\pm 588$, $p=0.00002$) from modern soils³¹.

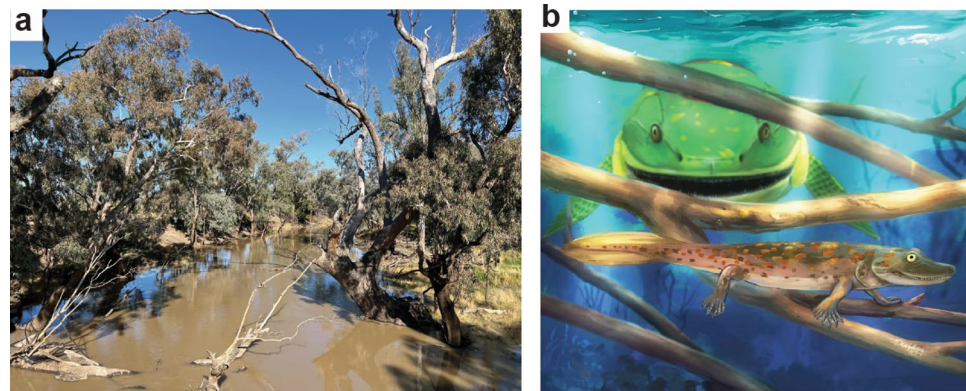


Figure 4. Analogous modern environment (a) and reconstruction of *Sinostega pani* (b); (a) Turragulla Creek, 4 km north of Pilliga, New South Wales, Australia. Pilliga box (*Eucalyptus pillagensis*) forms temperate dry woodland (MAP 571 mm, MAT 17.6 °C), and woody debris in the creek (S30.3049529° E148.8203385°), as an analogous modern environment for Chinese⁹ and Pennsylvanian¹² Late Devonian tetrapods. (b) reconstruction of *Sinostega pani*⁹ hiding from large *Hongyu chowi*¹⁴, behind woody debris. Reconstruction by Dinghua Yang.

$$S = 35.3D + 588 \quad (4)$$

Mean annual precipitation (*MAP* in mm) and mean annual temperature (*MAT* in °C) can be estimated for paleosols from chemical index of alteration without K_2O (*K* as $100Al_2O_3/[Al_2O_3 + CaO + Na_2O]$ in moles) and alkali index (*A*, as molar $K_2O + Na_2O/Al_2O_3$) of non-calcareous parts of paleosols³² by Eqs. 5 ($r^2 = 0.72$, $s.e. = \pm 182$ mm, $p = 0.00001$) and 6 ($r^2 = 0.37$, $s.e. = \pm 4.4$ °C, $p = 0.00001$).

$$MAP = 221.1e^{0.0197C} \quad (5)$$

$$MAT = -18.5S + 17.3 \quad (6)$$

Mean annual precipitation in calcareous soils of unconsolidated loess and alluvium of plains, can be inferred from depth to carbonate nodules (*D* in cm)³⁰ (*MAP* in mm) by Eq. 7 ($r^2 = 0.52$, $s.e. = \pm 147$ mm, $p = 0.00001$). Mean annual range of precipitation (*MARP* as mm difference between wettest and driest month mean) is related to the thickness of the Bk horizon (*H* in cm) of soils in unconsolidated sediment of plains, again with robust statistics ($r^2 = 0.58$, $s.e. = \pm 22$ mm, $p = 0.00001$), by Eq. 8.

$$MAP = 137.24 + 6.45D - 0.0132D^2 \quad (7)$$

$$MARP = 0.79H + 13.7 \quad (8)$$

Data availability

All data generated or analyzed during the current study are included in this published article and its supplementary information files, but GR can provide additional information on request (greg@uoregon.edu).

Received: 6 September 2023; Accepted: 17 November 2023

Published online: 21 November 2023

References

- Ahlberg, P. E. Follow the footprints and mind the gaps: A new look at the origin of tetrapods. *Earth Environ. Sci. Trans. Roy. Soc. Edinburgh* **109**, 115–137 (2018).
- Brusatte, S. L., O'Connor, J. K. & Jarvis, E. D. The origin and diversification of birds. *Curr. Biol.* **25**, 888–898 (2015).
- Almécija, S. *et al.* Fossil apes and human evolution. *Science* **372**, 4363 (2021).
- Clack, J. A. *Gaining Ground: The Origin and Evolution of Tetrapods* 400 (Indiana University Press, 2012).
- Retallack, G. J. & Huang, C. Ecology and evolution of Devonian trees in New York, USA. *Palaeogeogr. Palaeoclim. Palaeoec.* **299**, 110–128 (2011).
- Retallack, G. J. Woodland hypothesis for Devonian tetrapod evolution. *J. Geol.* **119**, 235–258 (2011).
- Romer, A. S. Tetrapod limbs and early tetrapod life. *Evolution* **12**, 365–369 (1958).
- Niedźwiedzki, G. *et al.* Tetrapod trackways from the early Middle Devonian period of Poland. *Nature* **463**, 43–48 (2010).
- Zhu, M. *et al.* First Devonian tetrapod from Asia. *Nature* **420**, 760–761 (2002).
- Lebedev, O. in *Fossil fishes as living systems* (ed. Mark-Kurik, E.) 265–272 (Talinn, Estonian Academy of Science, 1992).
- Blieck, A. *et al.* in *Devonian events and correlation* (eds Becker, R.T. & Kirchgasser, W.T.) 219–235 (Geol. Soc. London Spec. Publ. 278, 2007).
- Retallack, G. J., Hunt, R. R. & White, T. S. Late Devonian tetrapod habitats indicated by paleosols in Pennsylvania. *J. Geol. Soc. London* **166**, 1143–1156 (2009).
- Campbell, K. S. W. & Bell, M. W. A primitive amphibian from the Late Devonian of New South Wales. *Alcheringa* **1**, 369–381 (1977).
- Zhu, M., Ahlberg, P. E., Zhao, W. J. & Jia, L. T. A Devonian tetrapod-like fish reveals substantial parallelism in stem tetrapod evolution. *Nat. Ecol. Evol.* **1**, 1470–1476 (2017).
- Lebedev, O. L. A new tetrapod *Jakubsonia livnensis* from the Early Famennian (Devonian) of Russia and palaeoecological remarks on the Late Devonian tetrapod habitats. *Acta Univ. Latvi.* **679**, 79–98 (2004).
- Gess, R. W. & Ahlberg, P. E. A tetrapod fauna from within the Devonian Antarctic Circle. *Science* **360**, 1120–1124 (2018).
- Szrek, P. Vertebrates from the Upper Kellwasser Limestone, Frasnian-Famennian boundary beds (Upper Devonian of the Holy Cross Mountains (Poland)). *J. Verteb. Paleont.* **28**(suppl. 2), 150A (2008).
- Beznosov, P. A. *et al.* Morphology of the earliest reconstructable tetrapod *Parmastega aelidae*. *Nature* **574**, 527–531 (2019).
- Ahlberg, P. E. *Elginerpeton pancheni* and the earliest tetrapod clade. *Nature* **373**, 420–475 (1995).
- Shubin, N. H., Daeschler, E. B. & Jenkins, F. A. The pectoral fin of *Tiktaalik roseae* and the origin of the tetrapod limb. *Nature* **440**, 764–771 (2006).
- Long, J. A. *et al.* An exceptional Devonian fish from Australia sheds light on tetrapod origins. *Nature* **444**, 199–202 (2006).
- Boisvert, C. A. The pelvic fin and girdle of *Panderichthys* and the origin of tetrapod locomotion. *Nature* **438**, 1145–1147 (2005).
- Schultze, H. P. & Cloutier, R. (eds) *Devonian Fishes and Plants of Miguasha, Quebec, Canada* 374 (Pfeil, Munich, 1996).
- Pan, J. *et al.* *Continental Devonian System of Ningxia and Its Biotas* 237 (Geol. Publ. House, 1987).
- Pettitt, J. M. & Beck, C. B. *Archaeosperma arnoldii*—a cupulate seed from the Upper Devonian of North America. *Univ. Michigan Pap. Paleont.* **22**, 139–154 (1968).
- Ritchie, A. *et al.* The Sinolepidae, a family of antiarchs (placoderm fishes) from the Devonian of South China and eastern Australia. *Rec. Aust. Mus.* **44**, 319–370 (1992).
- Goedert, J. *et al.* Euryhaline ecology of early tetrapods revealed by stable isotopes. *Nature* **558**, 68–72 (2018).
- Guo, X. L. *et al.* Paleosols in Devonian red-beds from northwest China and their paleoclimatic characteristics. *Sediment. Geol.* **379**, 16–24 (2019).
- Todaeva, B. X. *Dunsianskii iazyk (Dongxiang Dictionary)* 151 (Izdatelstvo Vostochni Literaturi, 1961).
- Retallack, G. J. Pedogenic carbonate proxies for amount and seasonality of precipitation in paleosols. *Geology* **33**, 333–336 (2005).
- Breecker, D. O. & Retallack, G. J. Refining the pedogenic carbonate atmospheric CO₂ proxy and application to Miocene CO₂. *Palaeogeogr. Palaeoclim. Palaeoec.* **406**, 1–8 (2014).
- Sheldon, N. D., Retallack, G. J. & Tanaka, S. Geochemical climofunctions from North American soils and application to paleosols across the Eocene–Oligocene boundary in Oregon. *J. Geol.* **110**, 687–696 (2002).

33. Sheldon, N. D. & Retallack, G. J. Equation for compaction of paleosols due to burial. *Geology* **29**, 247–250 (2001).
34. Zhang, J., Zhang, B. & Zhao, H. Timing of amalgamation of the Alxa Block and the North China Block: Constraints based on detrital zircon U–Pb ages and sedimentologic and structural evidence. *Tectonophysics* **668**, 65–81 (2016).
35. Wu, M. *et al.* Characteristics of coal quality and element distribution in 9# coal seam of Renjiazhuang coal mine in Ningxia. *China Min. Mag.* **29**, 170–175 (2020).
36. Kalinowski, A. A. & Gurba, L. W. Interpretation of vitrinite reflectance–depth profiles in the Northern Denison Trough, Bowen Basin, Australia. *Int. J. Coal Geol.* **219**, 103367 (2020).
37. Lawesson, J. E. Some comments on the classification of African vegetation. *J. Vegetation Sci.* **5**, 441–444 (1994).
38. Zhao, X. *et al.* Silurian and Devonian paleomagnetic poles from North China and implications for Gondwana. *Earth Planet. Sci. Lett.* **117**, 497–506 (1993).
39. Retallack, G. J. Cambrian, Ordovician and Silurian pedostratigraphy and global events in Australia. *Aust. J. Earth Sci.* **56**, 571–586 (2009).
40. Retallack, G. J. Multiple Permian–Triassic life crises on land and at sea. *Glob. Planet. Change* **198**, 103415 (2021).
41. Retallack, G. J. Greenhouse crises of the past 300 million years. *Geol. Soc. Am. Bull.* **121**, 1441–1455 (2009).
42. Mao, X. G., Retallack, G. J. & Liu, X. M. Identification, characterization, and paleoclimatic implication of Early Cretaceous (Aptian–Albian) paleosol succession in Zhangye Danxia National Geopark, northwestern China. *Palaeogeogr. Palaeoclim. Palaeoec.* **601**, 111128 (2022).
43. van der Boon, A. *et al.* A persistent non-uniformitarian paleomagnetic field in the Devonian?. *Earth-Sci. Rev.* **231**, 104073 (2022).
44. Racki, G. A volcanic scenario for the Frasnian–Famennian major biotic crisis and other Late Devonian global changes: More answers than questions?. *Glob. Planet. Change* **189**, 103174 (2020).
45. Retallack, G. J. Soil carbon dioxide planetary thermostat. *Astrobiology* **22**, 116–123 (2022).
46. Pawlik, Ł *et al.* Impact of trees and forests on the Devonian landscape and weathering processes with implications to the global Earth's system properties—A critical review. *Earth-Sci. Rev.* **205**, 103200 (2020).
47. Lucas, S. G. *Thinopus* and a critical review of Devonian tetrapod footprints. *Ichnos* **22**, 136–154 (2015).
48. Qvarnström, M., Szrek, P., Ahlberg, P. E. & Niedźwiedzki, G. Non-marine paleoenvironment associated to the earliest tetrapod tracks. *Sci. Rep.* **8**, 1074 (2018).
49. Narkiewicz, M. & Retallack, G. J. Dolomitic paleosols in the lagoonal tetrapod track-bearing succession of the Holy Cross Mountains (Middle Devonian, Poland). *Sedim. Geol.* **299**, 74–87 (2014).
50. Stössel, I., Williams, E. A. & Higgs, K. T. Ichnology and depositional environment of the Middle Devonian Valentia Island tetrapod trackways, south-west Ireland. *Palaeogeogr. Palaeoclim. Palaeoec.* **462**, 16–40 (2016).
51. King, H. M. *et al.* Behavioral evidence for the evolution of walking and bounding before terrestriality in sarcopterygian fishes. *Proc. U.S. Nat. Acad. Sci.* **108**, 21146–21151 (2011).
52. Falkingham, P. L. & Horner, A. M. Trackways produced by lungfish during terrestrial locomotion. *Sci. Rep.* **6**, 1–10 (2016).
53. Stein, W. E. *et al.* Mid-Devonian *Archaeopteris* roots signal revolutionary change in earliest fossil forests. *Curr. Biol.* **30**, 421–431 (2020).
54. Baillie, B. R., Collier, K. J. & Nagels, J. Effects of forest harvesting and woody debris removal on two Northland streams, New Zealand. *N. Z. J. Mar. Freshw. Res.* **39**, 1–15 (2005).
55. Floyd, T. A., MacInnis, C. & Taylor, B. R. Effects of artificial woody structures on Atlantic salmon habitat and populations in a Nova Scotia stream. *River Res. Appl.* **25**, 272–282 (2009).
56. Hafis, A. W., Harrison, L. R., Utz, R. M. & Dunne, T. Quantifying the role of woody debris in providing bioenergetically favorable habitat for juvenile salmon. *Ecol. Mod.* **285**, 30–38 (2014).
57. Kenison, E. K., Litt, A. R., Pilliod, D. S. & McMahon, T. E. Role of habitat complexity in predator–prey dynamics between an introduced fish and larval ong-toed salamanders (*Ambystoma macrodactylum*). *Can. J. Zool.* **94**, 243–249 (2016).
58. Bylak, A. The effects of brown trout (*Salmo trutta morpha fario*) on habitat selection by larval Fire Salamanders (*Salamandra salamandra*): A predator-avoidance strategy. *Can. J. Zool.* **96**, 213–219 (2018).

Acknowledgements

Prof. Min Zhu and Wenjin Zhao graciously provided locality information for Shixiagou Canyon. Work was funded by National Science Foundation of China (Grant no. 41772168), the Natural Science Foundation of Gansu Province (Grant no. 20JR5RA272), the Second Tibetan Plateau Scientific Expedition and Research (STEP) program (2019QZKK0704), and the Programs for Foreign Talent (2022). For productive discussions, we thank Per Ahlberg, John Long, and Spencer Lucas.

Author contributions

X.G. and G.J.R. conceived the project, wrote and edited the manuscript jointly. X.G. secured funding for laboratory and field work. J.L. assisted X.G. and G.J.R. during fieldwork, and in the laboratory.

Competing interests

The authors declare no competing interests.

Additional information

Supplementary Information The online version contains supplementary material available at <https://doi.org/10.1038/s41598-023-47728-y>.

Correspondence and requests for materials should be addressed to G.J.R.

Reprints and permissions information is available at www.nature.com/reprints.

Publisher's note Springer Nature remains neutral with regard to jurisdictional claims in published maps and institutional affiliations.



Open Access This article is licensed under a Creative Commons Attribution 4.0 International License, which permits use, sharing, adaptation, distribution and reproduction in any medium or format, as long as you give appropriate credit to the original author(s) and the source, provide a link to the Creative Commons licence, and indicate if changes were made. The images or other third party material in this article are included in the article's Creative Commons licence, unless indicated otherwise in a credit line to the material. If material is not included in the article's Creative Commons licence and your intended use is not permitted by statutory regulation or exceeds the permitted use, you will need to obtain permission directly from the copyright holder. To view a copy of this licence, visit <http://creativecommons.org/licenses/by/4.0/>.

© The Author(s) 2023